Short Papers

Optimal Kinematic Design of 2-DOF Parallel Manipulators With Well-Shaped Workspace Bounded by a Specified Conditioning Index

Tian Huang, Meng Li, Zhanxian Li, Derek G. Chetwynd, and David J. Whitehouse

***Abstract*—This paper presents a hybrid method for the optimum kinematic design of two-degree-of-freedom (2-DOF) parallel manipulators with mirror symmetrical geometry. By taking advantage of both local and global approaches, the proposed method can be implemented in two steps. In the first step, the optimal architecture, in terms of isotropy and the behavior of the direct Jacobian matrix, is achieved, resulting in a set of closed-form parametric relationships that enable the number of design variables to be reduced. In the second step, the workspace bounded by the specified conditioning index is generated, which allows only one design parameter to be determined by optimizing a comprehensive index in a rectangular workspace. The kinematic optimization of a revolute-jointed 2-DOF parallel robot has been taken as an example to illustrate the effectiveness of this approach.**

***Index Terms*—Optimum design, parallel manipulators, performance index.**

I. Introduction

Kinematic design or dimensional synthesis is an important issue in the development of parallel manipulators because the performance of a system in terms of workspace, velocity, accuracy, and rigidity is dominated, to a great extent, by its geometrical characteristics. Kinematic design is primarily concerned with the determination of the dimensions of the geometric parameters and the range of the actuated joint variables, leading to, in general, optimizing a nonlinear cost function, subject to a set of appropriate constraints.

The approaches in previous work dealing with the kinematic design of parallel manipulators may be classified into two categories. One category is known as the local optimum design [2], [6], [10]–[12], [18], focusing upon finding the parametric loci necessary to generate a set of isotropy. Another category is referred to as the global optimum design [3], [5], [7], [14], [16], [17], attempting to optimize a global conditioning index. The typical work in this phase was proposed by Gosselin and Angeles [7], in which a global conditioning index represented by the mean value of the reciprocal of conditioning number of the Jacobian was used as a cost function for maximization. The reasons for having to implement a global approach are: 1) the condition necessary to generate an isotropy is unable to provide sufficient design constraints to achieve a unique solution; and 2) the global kinematic performance could not be guaranteed simply by conducting local optimum design. For this reason, the global optimal method has been well accepted and widely employed for the evaluation of the kinematic performance of existing parallel manipulators and/or for optimization of new machines. Although the global approach is very general and meaningful in practice, it cannot be implemented analytically, especially when a number of design variables are involved.

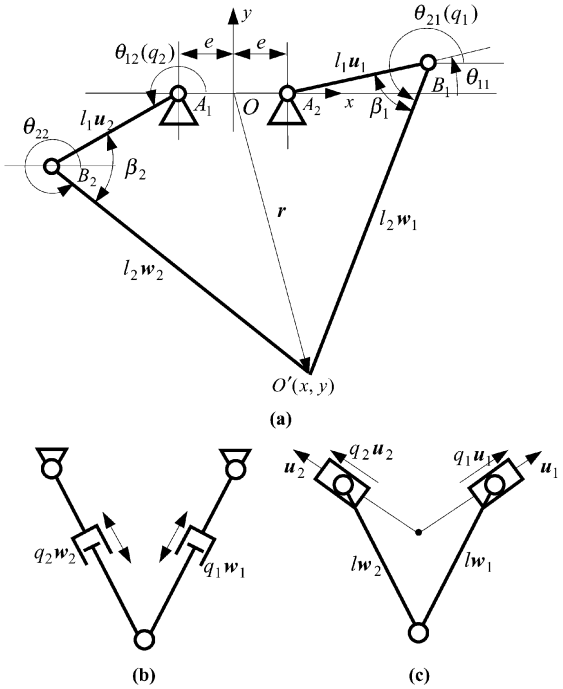

Fig. 1. 2-DOF parallel robots with mirror symmetrical geometry. (a) Proximal arm type. (b) Telescopic leg type. (c) Linear drive type.

By taking advantage of both local and global optimal approaches, this paper presents a hybrid method that enables the optimal kinematic design to be implemented by two steps. In the first step, the optimal architecture is achieved, resulting in a set of closed-form parametric relationships. In the second step, the workspace bounded by the specified conditioning index is generated, which allows a well-shaped and conditioned workspace to be obtained via optimizing a comprehensive index. A revolute-jointed two-degree-of-freedom (2-DOF) parallel robot will be taken as an example to demonstrate the effectiveness of this approach.

II. Kinematic Equations

As shown in Fig. 1(a), the example object of study is a 2-DOF parallel robot with mirror symmetrical geometry. The robot is revolute jointed and driven by two proximal arms connected with the frame by the fixed revolute joints. Although discussion here will concentrate on this type of robot, similar robots, either internally driven by two telescopic legs or externally driven by two linear drives, as shown in Fig. 1(b) and (c), can be dealt with in the same way.

In order to evaluate the kinematic performance, the inverse position and velocity analyses should be carried out. In the $O - xy$ coordinate

Manuscript received November 22, 2002; revised May 15, 2003. This paper was recommended for publication by Associate Editor J. Merlet and Editor I. Walker upon evaluation of the reviewers' comments. This work was supported in part by the "863" Development Scheme under Grant 2001AA421220, in part by the National Science Foundation of China under Grant 50075059, in part by the Royal Society UK–China Joint Research under Grant Q820, and in part by the Education Ministry of China.

T. Huang, M. Li, and Z. Li are with the School of Mechanical Engineering, Tianjin University, Tianjin 300072, China (e-mail: htiantju@public.tpt.tj.cn; th@eng.warwick.ac.uk).

D. G. Chetwynd and D. J. Whitehouse are with the School of Engineering, The University of Warwick, Coventry CV4 7AL, U.K.

Digital Object Identifier 10.1109/TRA.2004.824690

system shown in Fig. 1(a), the closed-loop constraint equation can be written as

$$\boldsymbol{r} - \mathrm{sgn}(i)e\boldsymbol{e}_1 - l_1\boldsymbol{u}_i = l_2\boldsymbol{w}_i, \quad i = 1, 2 \tag{1}$$

where $\boldsymbol{r} = (\,x \quad y\,)^T$ is the position vector of the reference point O' of the end-effector; l_1, l_2, $\boldsymbol{u}_i$, and $\boldsymbol{w}_i$ are the lengths and unit vectors of the proximal and distal links; e is the distance between O and the axis of the actuated joint; and

$$\boldsymbol{u}_i = (\,\cos\theta_{1i} \quad \sin\theta_{1i}\,)^T, \quad \boldsymbol{w}_i = (\,\cos\theta_{2i} \quad \sin\theta_{2i}\,)^T$$
$$\boldsymbol{e}_1 = (\,1 \quad 0\,)^T, \quad \mathrm{sgn}(i) = \begin{cases} 1, & i = 1 \\ -1, & i = 2 \end{cases}$$

where θ_{1i} (or q_i) and θ_{2i} are the position angles of the proximal and distal links, respectively.

Taking dot product on both sides of (1) and adding the assembly mode gives the solution to

$$\theta_{1i} = 2\arctan\frac{-A_i + \mathrm{sgn}(i)\sqrt{A_i^2 - C_i^2 + B_i^2}}{C_i - B_i} \tag{2}$$

where

$$A_i = -2l_1 y$$
$$B_i = -2l_1(x - \mathrm{sgn}(i)e)$$
$$C_i = x^2 + y^2 + e^2 + l_1^2 - l_2^2 - 2\mathrm{sgn}(i)ex.$$

Thus, $\boldsymbol{u}_i$ can be determined, and from (1)

$$\boldsymbol{w}_i = \frac{(\boldsymbol{r} - \mathrm{sgn}(i)e\boldsymbol{e}_1 - l_1\boldsymbol{u}_i)}{l_2}.$$

Differentiating (1) with respect to time yields

$$\boldsymbol{v} = l_1\dot{\theta}_{1i}\boldsymbol{Q}\boldsymbol{u}_i + l_2\dot{\theta}_{2i}\boldsymbol{Q}\boldsymbol{w}_i \tag{3}$$

where $\boldsymbol{Q} = \begin{bmatrix} 0 & -1 \\ 1 & 0 \end{bmatrix}$.

Without loss of generality, let the proximal link have a unit length, i.e., $l_1 = 1$ and replace $\dot{\theta}_{1i}$ by $\dot{q}_i$. Multiplying both sides of (3) by $\boldsymbol{w}_i^T$ and rewriting in matrix form yields the general structure of the velocity mapping function of the 2-DOF parallel robots shown in Fig. 1

$$\dot{\boldsymbol{q}} = \boldsymbol{A}^{-1}\boldsymbol{B}\boldsymbol{v} = \boldsymbol{J}\boldsymbol{v}, \quad \dot{\boldsymbol{q}} = (\dot{q}_1 \;\; \dot{q}_2)^T \tag{4}$$

where $\boldsymbol{J}$ is the Jacobian and $\boldsymbol{A}$, $\boldsymbol{B}$ are known as the direct and indirect Jacobian matrices [3], respectively

$$\boldsymbol{A} = \begin{cases} \mathrm{diag}\left[\boldsymbol{w}_i^T\boldsymbol{Q}\boldsymbol{u}_i\right], & \text{proximal arm type} \\ \boldsymbol{E}_2, & \text{telescopic leg type} \\ \mathrm{diag}\left[\boldsymbol{w}_i^T\boldsymbol{u}_i\right], & \text{linear drive type} \end{cases}, \quad \boldsymbol{B} = [\boldsymbol{w}_1\;\boldsymbol{w}_2]^T.$$

$\boldsymbol{E}_2$ is a unit matrix.

III. Optimum Design

A. Proposed Idea

It has been well accepted that the most suitable local performance index is the condition number of the Jacobian [15]. Isotropy has also been used as a design criterion to find the optimal configuration [2], [6]–[10], [18]. That is a configuration at which the condition number of the Jacobian reaches its minimum value in the overall workspace. Therefore, a parallel robot must behave well at the optimal configuration, in terms of isotropy. This will allow a hybrid approach to be developed that can be implemented in two steps. The first step of this approach aims at formulating a set of closed-form parametric relationships necessary to obtain an optimal configuration, in terms of the isotropy and the force-transmission behavior. Then, the second step involves determining the independent kinematic parameters by optimizing a global index in a well-shaped workspace bounded by the specified conditioning index.

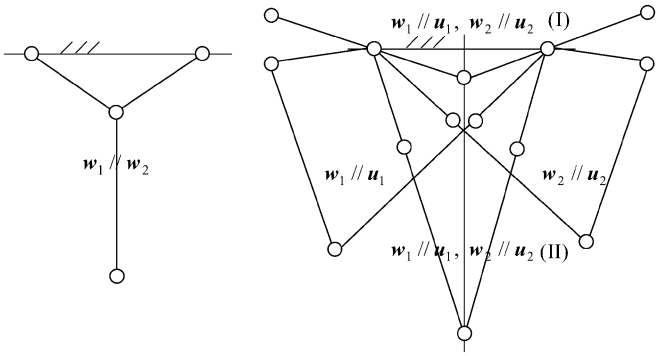

Fig. 2. Singular configurations of the example robot.

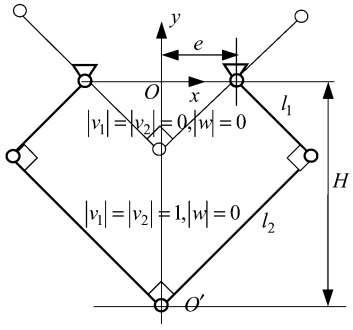

Fig. 3. Isotropic configurations.

B. Local Optimum Design

1) Conditioning Index: Following the notation used by [7], the conditioning index is defined by

$$0 \le \frac{1}{\kappa} = \frac{\sigma_1}{\sigma_2} \le 1 \tag{5}$$

where κ, σ_1, and σ_2 are the condition number, and the minimum and maximum singular values of the Jacobian. For the example parallel robot, we have

$$\sigma_{1,2} = \frac{1}{\sqrt{2}|v_1||v_2|}\left(\left(v_1^2 + v_2^2\right) \mp \left(\left(v_1^2 - v_2^2\right)^2 + (2v_1v_2w)^2\right)^{1/2}\right)^{1/2} \tag{6}$$

$$\frac{1}{\kappa} = \frac{\sigma_1}{\sigma_2} = \left(\frac{\left(v_1^2 + v_2^2\right) - \left(\left(v_1^2 - v_2^2\right)^2 + (2v_1v_2w)^2\right)^{1/2}}{\left(v_1^2 + v_2^2\right) + \left(\left(v_1^2 - v_2^2\right)^2 + (2v_1v_2w)^2\right)^{1/2}}\right)^{1/2} \tag{7}$$

where

$$v_i^2 = \left(\boldsymbol{w}_i^T\boldsymbol{Q}\boldsymbol{u}_i\right)^2 = 1 - \left(\boldsymbol{w}_i^T\boldsymbol{u}_i\right)^2 = 1 - \cos^2\beta_i$$
$$|w| = \left|\boldsymbol{w}_1^T\boldsymbol{w}_2\right| \tag{8}$$

and $\beta_i = \arccos\left|\boldsymbol{w}_i^T\boldsymbol{u}_i\right|$ is the acute angle (pressure angle) between the proximal and distal links in the ith kinematic chain [see Fig. 1(a)], representing the force-transmission behavior of the robot.

2) Singularity and Optimal Configuration: By observing (7) and Fig. 2, it is easy to see in the following cases where the singularity occurs.

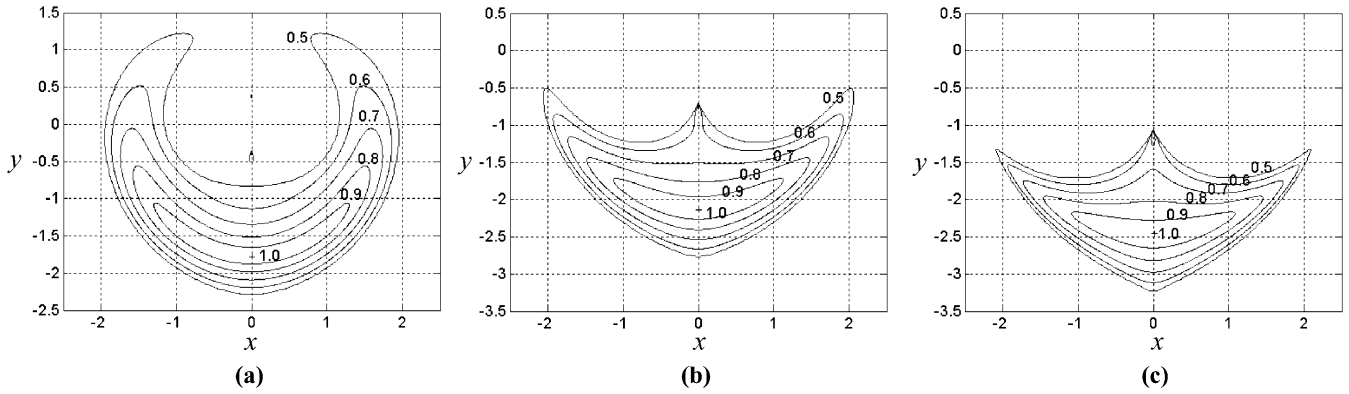

Fig. 4. Contours of $1/\kappa$ versus δ in workspace bounded by $1/\kappa_0 = 0.5$. (a) $\delta = 1.5$. (b) $\delta = 2.0$. (c) $\delta = 2.5$.

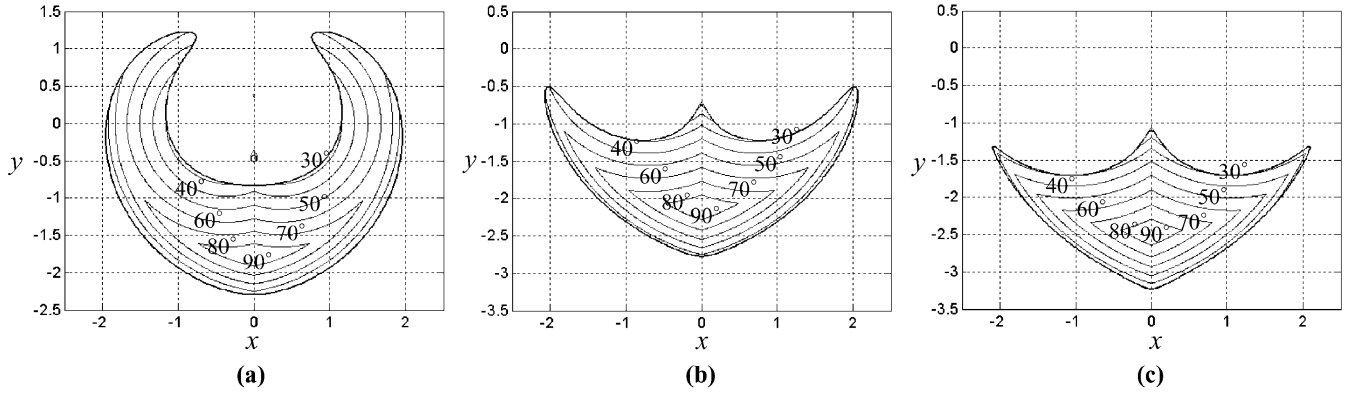

Fig. 5. Contours of $\beta_{\min}$ versus δ in workspace bounded by $1/\kappa_0 = 0.5$. (a) $\delta = 1.5$. (b) $\delta = 2.0$. (c) $\delta = 2.5$.

Case 1) If $|w| \to 1 (\boldsymbol{w}_1 // \boldsymbol{w}_2)$, then $1/\kappa \to 0$.
Case 2) If either $|v_1| \to 0 (\boldsymbol{w}_1 // \boldsymbol{u}_1)$ or $|v_2| \to 0 (\boldsymbol{w}_2 // \boldsymbol{u}_2)$ but not both, then $(1/\kappa \to 0)$.
Case 3) If $|v_1| = |v_2| = v_c$, (7) gives

$$\frac{1}{\kappa} = \left(\frac{1-|w|}{1+|w|}\right)^{1/2}. \tag{9}$$

Thus, $1/\kappa \neq 0$ unless $|w| \to 1$. In this case, however, if $|v_1| \to 0$ and $|v_2| \to 0$, then (6) gives $\sigma_1 = \sigma_2 \to \infty$, leading to the singularity due to the degeneration of the direct Jacobian.

The necessary condition for achieving an isotropy is that (7) has two identical roots, such that

$$|w| = 0, \quad |v_1| = |v_2|. \tag{10}$$

In particular, when $|v_1| = |v_2| = 1$, (7) gives $1/\kappa = 1$, and the corresponding isotropic configuration is a pentagon with three right corner angles (see Fig. 3). However, when $|v_1| = |v_2| = 0$, (9) also gives $1/\kappa = 1$, and the isotropic configuration turns out to be a right triangle (see Fig. 3). Referring back to (6), it is clear that the former case gives $\sigma_1 = \sigma_2 = 1$, while the latter leads to $\sigma_1 = \sigma_2 \to \infty$. Therefore, the so-called optimal configuration should be that at which σ_1 takes the maximum and σ_2 takes the minimum values simultaneously in the overall workspace.

According to the above analysis, the conditions for the example robot to achieve an optimal configuration are

$$|w| = 0, \quad |v_1| = |v_2| = 1. \tag{11}$$

Obviously, the conditions given in (11) are also suitable for the other two parallel robots shown in Fig. 1(b) and (c), depending upon the corresponding $|v_i|$.

For the example robot, (11) will produce a set of parametric relationships as follows:

$$H = \frac{\sqrt{2}}{2}(l_1 + l_2), \quad e = \frac{\sqrt{2}}{2}(l_2 - l_1) \tag{12}$$

where H is the distance from O to O' when the robot is at the optimal configuration (see Fig. 3).

C. Global Optimum Design

1) Observations and Discussions: (1) Let δ be the ratio of l_2 to l_1. This means that the parametric relationships given by (12) leave only one independent geometric parameter, δ, to be determined as $l_1 = 1$. In order to achieve a robot having a relatively large yet well-conditioned workspace, it is necessary in the first place to gain an insight into the influence of δ on the location, shape, and size of the workspace bounded by a specified conditioning index $1/\kappa_0$. Here, this set of workspaces is defined as $W_{\kappa 0}$ with each element $W_{\kappa 0}(\delta) \in W_{\kappa 0}$ being associated with a given δ. Given $1/\kappa_0$ and δ, the boundary of $W_{\kappa 0}(\delta)$ can be found using the 1-D root search algorithm, the golden-section method, for example. It is worth pointing out, however, that for the systems with higher DOFs, it is necessary to develop an effective algorithm to find the boundary bounded by the specified $1/\kappa_0$.

Fig. 4 shows the contours representing the variations in shape, size, and location of $W_{\kappa 0}(\delta)$ versus changes in $\delta = 1.5$–2.5 and $1/\kappa_0 = 0.5$–1.0. It can be seen that the shape of $W_{\kappa 0}(\delta)$ is similar to the reachable workspace of the robot of this type [1]. Meanwhile, the distance from the "center" of $W_{\kappa 0}(\delta)$ to O increases with the increase of δ, and

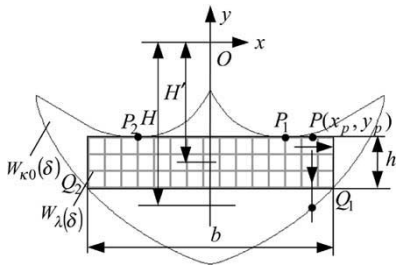

Fig. 6. 1-D search for the maximum rectangular workspace in $W_{\kappa 0}(\delta)$.

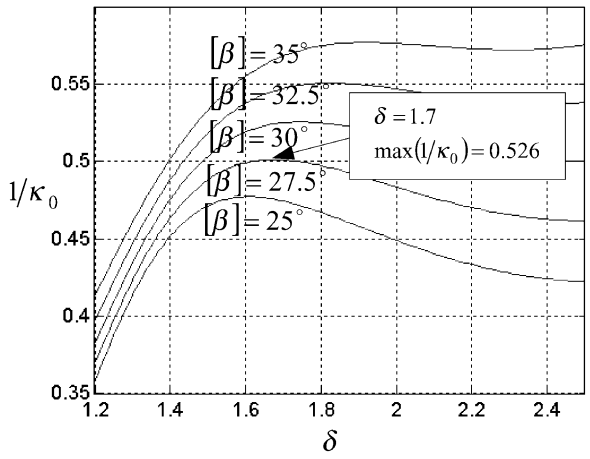

Fig. 7. Variation of $1/\kappa_0$ versus $[\beta]$ and δ.

increasing $1/\kappa_0$ reduces the size of $W_{\kappa 0}(\delta)$, meaning that to achieve a better-conditioned robot must be at the cost of size of workspace. Fig. 4 also shows that the area of $W_{\kappa 0}(\delta)$ bounded by a given $1/\kappa_0$ deceases with the increase in δ, but this tendency becomes weaker when $\delta > 2.0$. Fig. 5 shows the contours representing the variations of the minimum pressure angle $\beta_{\min} = \min(\beta_1 \quad \beta_2)$ versus changes in $\delta = 1.5$–2.5 in $W_{\kappa 0}(\delta)$ bounded by $1/\kappa_0 = 0.5$–1.0. It can be seen that the distribution pattern of $\beta_{\min}$ appears to be closely similar to that of $1/\kappa$. For example, the contour associated with $\beta_{\min} = 30^\circ$ approximately matches that associated with $1/\kappa_0 = 0.5$. Meanwhile, $\beta_{\min}$ always takes the minimum value on the upper bound of $W_{\kappa 0}(\delta)$, regardless of what value δ may take. These observations indeed provide us with some important information for the global optimum design in what follows.

2) Global Performance Index: From an application point of view, it is more meaningful for the example robot to possess a well-shaped workspace that can be tailored out of $W_{\kappa 0}(\delta)$ for a given $1/\kappa_0$. A rectangular workspace $W_\lambda(\delta)$ with fixed width/height ratio $\lambda = b/h$ might be typically the first priority. As shown in Fig. 6, $W_\lambda(\delta)$ is defined in such a way that it is tangential to the upper bound of $W_{\kappa 0}(\delta)$ at the points P_1 and P_2, and intersects with the lower bound of $W_{\kappa 0}(\delta)$ at the corners Q_1 and Q_2, respectively. In this case, a global and comprehensive performance index for determining δ is proposed as an objective function for maximization. This index can be represented by

$$\eta = \frac{\Delta_s}{\bar{\kappa}} \rightarrow \max \tag{13}$$

where $1/\bar{\kappa}$ is the mean value of the conditioning index $1/\kappa$ evaluated in $W_\lambda(\delta)$; $\Delta_s = S/S_{\max}$, and S is the area of $W_\lambda(\delta)$, $S_{\max}$ is the maximum value of S when δ varies in the range of $1 \le \delta \le \delta_{\max}$. Here, $\delta_{\max} = 2.5$ is suggested for a practical design. The index proposed here is a modified version of the global conditioning index proposed

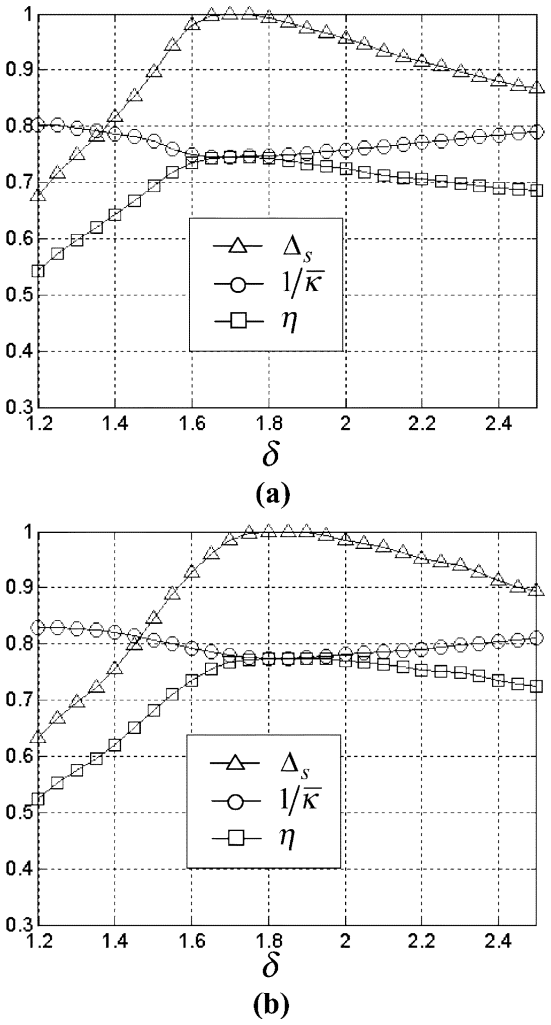

Fig. 8. Performance indexes versus δ. (a) $1/\kappa_0 = 0.256$. (b) $1/\kappa_0 = 0.581$ with $\lambda = 4$.

TABLE I
RESULTS OF OPTIMIZATION WITH $\lambda = 4$

	$1/\kappa_0 = 0.526$	$1/\kappa_0 = 0.581$
l_2	1.7	1.85
e	0.4950	0.6001
h	0.7322	0.6667
H'	1.3056	1.5178
$1/\bar{\kappa}$	0.7444	0.8004
S	2.0354	1.7778
η	0.7453	0.8004

in [7]. In computer implementation, $1/\bar{\kappa}$ can be numerically calculated by

$$\frac{1}{\bar{\kappa}} = \frac{1}{M \times N} \sum_{m=1}^{M} \sum_{n=1}^{N} \frac{1}{\kappa_{mn}} \tag{14}$$

where $\kappa_{mn} \ge \kappa_0$ is the value of κ at node $(m \quad n)$ of $(M-1) \times (N-1)$ equally meshed $W_{\kappa 0}(\delta)$. In order to choose the right value of the conditioning limit $1/\kappa_0$, the force-transmission behavior should be considered. $1/\kappa_0$ can be determined such that $\min(\beta_{\min}) \ge [\beta]$ in

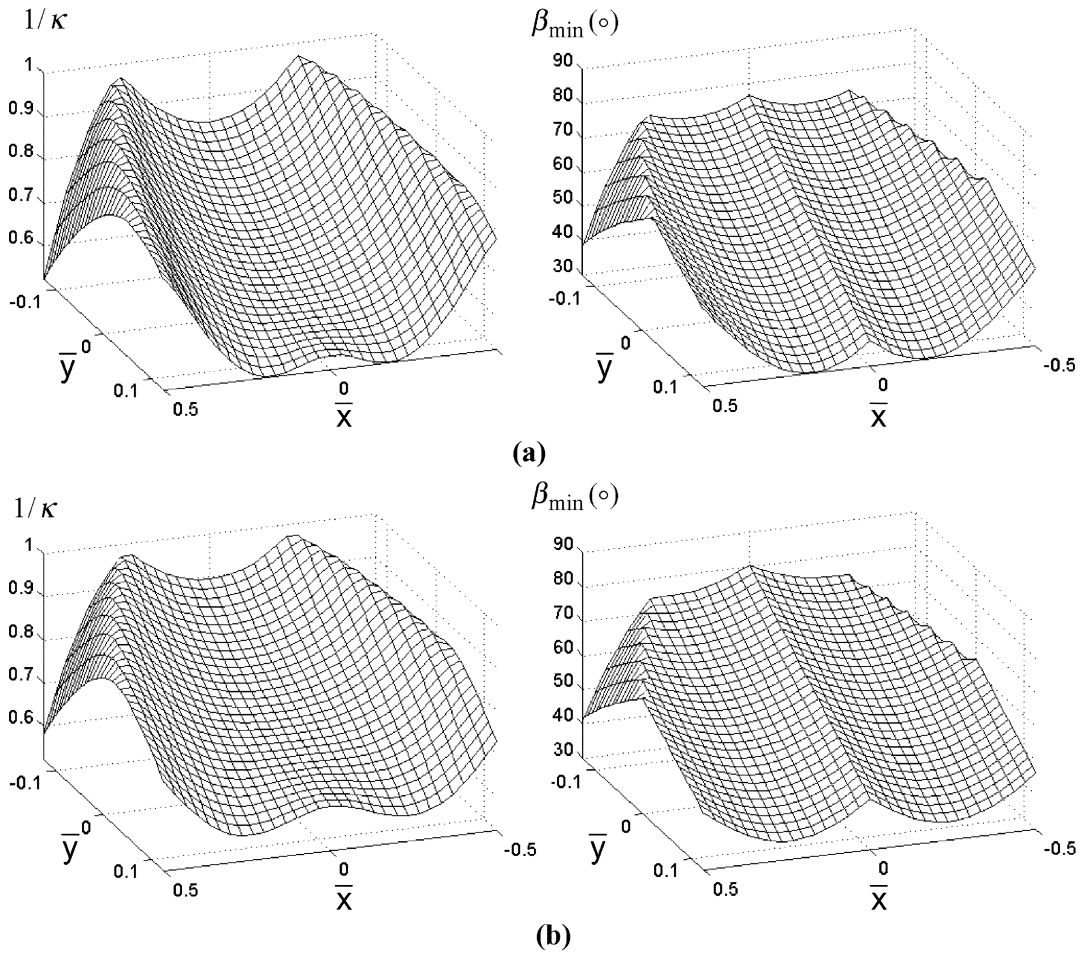

Fig. 9. $1/\kappa$ and $\beta_{\min}$ distributions in a normalized rectangular workspace. (a) $1/\kappa_0 = 0.526$, $\delta = 1.7$. (b) $1/\kappa_0 = 0.581$, $\delta = 1.85$ with $\lambda = 4$.

$W_\lambda(\delta)$, with $[\beta]$ being a prescribed allowable pressure angle. In practice, $[\beta] = 30°$–$35°$ would be a reasonable choice. It can be seen from Fig. 1(a) that the pressure angle β_i can be expressed by

$$\beta_i = \arccos \frac{1}{2\delta} \left| 1 + \delta^2 - (x - \operatorname{sgn}(i)e)^2 - y^2 \right| \tag{15}$$

where

$$-\frac{1}{2}b \le x \le \frac{1}{2}b, \quad -\frac{1}{2}h - H' \le y \le \frac{1}{2}h - H', \quad \lambda = \frac{b}{h}$$

and H' denotes the distance from the center of $W_\lambda(\delta)$ to the point O. Observation of (15) indicates that β_i takes the minimum value in $W_\lambda(\delta)$ when O' is located at

$$x_0 = \begin{cases} e, & i = 1 \\ -e, & i = 2 \end{cases} \qquad y_0 = \frac{h}{2} - H'. \tag{16}$$

Substituting (16) into (15) and replacing β_i in (15) by $[\beta]$, leads to

$$x_0 = \pm e, \quad y_0 = -(1 + \delta^2 - 2\delta \cos[\beta])^{1/2}. \tag{17}$$

This allows $1/\kappa_0$ to be determined using (7). Fig. 7 shows the variation of $1/\kappa_0$ versus changes in $[\beta]$ and δ. Therefore, $\max(1/\kappa_0)$ can be used as the conditioning limit for $1 \le \delta \le \delta_{\max}$. For example, if $[\beta] = 30°$, then $\max(1/\kappa_0) = 0.526$, as shown in Fig. 7.

In addition, referring back to Fig. 6, a numerical algorithm can be developed for searching S as follows.

1) Given δ and $[\beta]$, generate the boundary of $W_{\kappa 0}(\delta)$ bounded by $\max(1/\kappa_0)$.
2) Move O' along the x axis to the tangential point $P(x_P, y_P)$ of $W_{\kappa 0}(\delta)$, with the point P_1 being the starting point. Then, move O' along the $-y$ axis in an iterative manner to the point $Q(x_Q = x_P, y_Q)$ located on the lower bound of $W_{\kappa 0}(\delta)$ until

$$\left| \frac{2x_P}{(y_P - y_Q) - \lambda} \right| < \varepsilon \tag{18}$$

where ε is the accuracy of convergence. In this way, the width b, height h, of $W_\lambda(\delta)$, and distance H' from its center to the point O can be found by

$$b = 2x_P, \quad h = y_P - y_Q, \quad H' = -y_P + \frac{h}{2}. \tag{19}$$

The golden-section method can also be employed for this purpose.

IV. Examples

Given $\lambda = 4$, two cases associated with $1/\kappa_0 = 0.526$ ($[\beta] = 30°$) and $1/\kappa_0 = 0.581$ ($[\beta] = 35°$) have been considered as examples for the optimum kinematic design of the robot. Fig. 8 shows the variations of Δ_s, $1/\bar{\kappa}$, and η versus δ. It can be seen from Fig. 8(a) that in the first case, $1/\bar{\kappa}$ varies slightly between 0.74 and 0.80, while Δ_s takes the maximum value at $\delta = 1.7$, resulting in the maximum value of η at the same δ. The same rule is followed by the second case [see Fig. 8(b)] where $1/\bar{\kappa}$ varies between 0.77 and 0.83, while η takes the maximum

value at $\delta = 1.85$. An interesting observation is that for a given $[\beta]$, the δ for $1/\kappa_0$ to take the maximum value is identical to that for η to do the same. The results of optimization of both cases are given in Table I. By taking the coordinate transformation

$$\bar{x} = \frac{x}{b}, \quad \bar{y} = \frac{(y + H')}{b}.$$

Fig. 9 shows the distributions of $1/\kappa$ and $\beta_{\min}$ in the normalized workspace $W_\lambda(\delta)$. It can be seen that for both cases, the boundary of W_λ is strictly bounded by the specified $1/\kappa_0$ at four points, and the minimum value of $\beta_{\min}$ in the entire workspace equals $[\beta]$, as expected. This means that bounded by the conditioning index, a relatively large, yet well-behaved, workspace of the robot can be achieved by using this approach. Meanwhile, the computation results also show that λ has little bearing on the optimized δ, meaning that any rectangular workspace having guaranteed performance can be tailed out of the $W_{\kappa 0}(\delta)$.

V. Conclusions

This paper presents a hybrid method for the optimum design of a 2-DOF parallel manipulator. The conclusions are drawn as follows.

1) A set of closed-form parametric relationships has been found for generating an optimal architecture, using the isotropic condition and a maximization of the coefficient appearing in the direct Jacobian matrix. This allows only one parameter to be determined in the global optimum design.
2) A modified global index is proposed. Maximization of this index enables one to achieve a relatively large, yet well-conditioned, rectangular workspace bounded by the conditioning limit $1/\kappa_0$, which can be determined by a specified allowable pressure angle $[\beta]$.
3) The width/height ratio λ has little bearing on the optimized δ, allowing any rectangular workspace having guaranteed good performance to be tailed out of the $W/\kappa_0(\delta)$.
4) For the right use of the proposed method to the optimal design of other robots that might be a mix between translational and rotational DOFs, the normalization technique should be considered so as to allow the entries of the Jacobian matrix to have the same dimensions.

References

[1] J. J. Cervantez-Sanchez and J. G. A. Rendon-Sanchez, "Simplified approach for obtaining the workspace of a class of 2-DOF planar parallel robots," *Mech. Mach. Theory*, vol. 34, no. 7, pp. 1057–1073, 1999.

[2] D. Chablat, P. Wenger, and J. Angeles, "The iso-conditioning loci of a class of closed-chain manipulators," in *Proc. IEEE Int. Conf. Robotics and Automation*, Leuven, Belgium, 1998, pp. 1970–1975.

[3] J. Duffy, *Static and Kinematics With Application to Robotics*. Cambridge, U.K.: Cambridge Univ. Press, 1996.

[4] F. Gao, "A physical model of the solution space and the atlas of the reachable workspace for 2-DOF parallel planar manipulators," *Mech. Mach. Theory*, vol. 31, no. 2, pp. 173–184, 1996.

[5] F. Gao and X. Liu, "Performance evaluation of 2-DOF planar parallel robots," *Mech. Mach. Theory*, vol. 33, no. 6, pp. 661–668, 1998.

[6] C. M. Gosselin and J. Angeles, "The optimum kinematic design of a spherical 3-DOF parallel manipulator," *ASME J. Mech., Transm., Automat. Des.*, vol. 111, no. 2, pp. 202–207, 1989.

[7] C. M. Gosselin and J. Angeles, "A globe performance index for the kinematic optimization of robotic manipulators," *ASME J. Mech. Des.*, vol. 113, no. 3, pp. 220–226, 1991.

[8] C. M. Gosselin, "The optimum design of robotic manipulators using dexterity indexes," *J. Robot. Auton. Syst.*, vol. 9, no. 4, pp. 213–226, 1993.

[9] C. M. Gosselin and J. Wang, "Singularity loci of planar parallel manipulators with revolute actuators," *Robot. Auton. Syst.*, vol. 21, no. 4, pp. 377–398, 1997.

[10] T. Huang, D. J. Whitehouse, and J. S. Wang, "Local dexterity, optimum architecture and design criteria of parallel machine tools," *CIRP Ann.*, vol. 47, no. 1, pp. 347–351, 1998.

[11] T. Huang, J. S. Wang, and D. J. Whitehouse, "Theory and methodology for kinematic design of Gough–Stewart platforms," *Sci. China*, ser. (E), vol. 42, no. 4, pp. 425–436, 1999.

[12] T. Huang, J. S. Wang, C. M. Gosselin, and D. J. Whitehouse, "Kinematic synthesis of hexapods with prescribed orientation capability and well-conditioned dexterity," *SME J. Manufact. Processes*, vol. 2, no. 1, pp. 36–47, 1999.

[13] M. G. Mohamed and J. Duffy, "A direct determination of the instantaneous kinematics of fully parallel robot manipulators," *ASME J. Mech. Des.*, vol. 107, no. 2, pp. 226–273, 1985.

[14] J. R. Singh and J. Rastegar, "Optimal synthesis of robot manipulators based on global kinematic parameters," *Mech. Mach. Theory*, vol. 30, no. 4, pp. 569–580, 1995.

[15] J. K. Salisbury and J. J. Craig, "Artificial hands: Force control and kinematic issues," *Int. J. Robot. Res.*, vol. 1, no. 1, pp. 4–17, 1983.

[16] L. Stocco, S. E. Salcudean, and F. Sassani, "Fast constrained global minimax optimization of robot parameters," *Robotica*, vol. 16, no. 6, pp. 595–605, 1998.

[17] L. W. Tsai and S. Joshi, "Kinematics and optimization of a 3UPU parallel manipulator," *ASME J. Mech. Des.*, vol. 122, no. 4, pp. 439–446, 2002.

[18] K. Zanganeh and J. Angeles, "Kinematic isotropy and the optimum design of parallel manipulators," *Int. J. Robot. Res.*, vol. 6, no. 2, pp. 185–197, 1997.

A Numerical Test for the Closure Properties of 3-D Grasps

Xiangyang Zhu, Han Ding, *Senior Member, IEEE*, and Michael Y. Wang, *Member, IEEE*

***Abstract*—This paper presents a numerical test for the closure properties (force closure and form closure) of multifingered grasps. For three-dimensional (3-D) grasps with frictional point contacts or soft contacts, the numerical test is formulated as a convex constrained optimization problem without linearization of the friction cone. For 3-D frictionless grasps, it can be calculated by solving a single linear program. The proposed numerical test (along with the rank of the grasp matrix) provides an efficient tool for the analysis of the force-closure property and the relative force-closure property.**

***Index Terms*—Multifingered grasp, numerical test, (relative) force closure.**

I. Introduction

As one of the fundamental issues of multifingered grasping and dexterous manipulation, *form-closure* and *force-closure* analysis was extensively investigated in the context of robotics [1]–[30]. The

Manuscript received May 19, 2003. This paper was recommended for publication by Associate Editor I. Kao and Editor I. Walker upon evaluation of the reviewers' comments. This work was supported by the National Natural Science Foundation of China under Grants 50175014 and 50390063.

X. Zhu and H. Ding are with the Robotics Institute, School of Mechanical Engineering, Shanghai Jiaotong University, Shanghai 200030, China (e-mail: mexyzhu@sjtu.edu.cn; hding@sjtu.edu.cn).

M. Y. Wang is with the Department of Automation and Computer-Aided Engineering, The Chinese University of Hong Kong, Shatin, NT, Hong Kong (e-mail: yuwang@acae.cuhk.edu.hk).

Digital Object Identifier 10.1109/TRA.2004.825514